Hindawi
Shock and Vibration
Volume 2017, Article ID 8628671, 10 pages
https://doi.org/10.1155/2017/8628671

Research Article

Numerical Evaluation on Dynamic Response of Existing Underlying Tunnel Induced by Blasting Excavation of a Subway Tunnel

Jixue Zhou,[1,2,3] Yi Luo,[1] XinPing Li,[1] Yunhua Guo,[1] and Tingting Liu[1]

[1]*Hubei Key Laboratory of Roadway Bridge & Structure, Wuhan University of Technology, No. 122 Luoshi Rd., Wuhan 430070, China*
[2]*School of Civil Engineering and Architecture, Wuhan University of Technology, No. 122 Luoshi Rd., Wuhan 430070, China*
[3]*China Railway 20 Bureau Group Co., Ltd., No. 89 Taihua Road, Xi'an 710016, China*

Correspondence should be addressed to Yi Luo; yluo@whut.edu.cn

Received 1 April 2017; Accepted 7 May 2017; Published 19 June 2017

Academic Editor: Abdul Qadir Bhatti

In Southwest China, most regions are mountainous, where traditional drill-and-blast method is adopted to excavate relatively harder rocks. However, blasting would cause vibration to adjacent structures and might result in damage or even failure. This paper considers a case where subway tunnel is overlying an existing railway tunnel, while the excavation requires blasting method. Vibration and stress distribution are calculated via Dynamic Finite Element Method (DFEM) for both full-face excavation and CD method. Result shows that vibration induced by CD method is only 28% of that caused by full-face blasting with same distance. Peak vibration is located on the lining facing the blasting source, while peak tensile stress is on the other side of the contour due to the reflection of stress wave on strata boundary. And peak value of tensile stress induced by full-face blasting is capable of causing lining failure; thus full-face blasting is not suggested within 40 m beyond the underlying tunnel axis. However, CD method has shown much advantage, since blasting within 25 m is also considered safe to the underlying tunnel. But when the blasting source is as near as 12 m within the underlying tunnel, the CD method is no longer safe.

1. Introduction

World population growth is encouraging massive request on convenient traffic and large residential settlement, which results in fast development in subway system [1, 2]. For example, more than 410 km subway is in operation beneath London, UK [3], and 293 km beneath Madrid, Spain [4]. Developed regions such as Hong Kong are making good use of their underground space for not only subway tunnels but also other underground caverns [5], which makes it common to have different tunnels or underground spaces overlapping each other at different elevations. Similar situations are also encountered in fast developing cities in China during recent years, while great investments are made in subway construction before cities are too crowded.

Usually, the subway tunneling is achieved by shield machines [6, 7], but due to the turning curvature limitation and geological or economical issues, the drill-and-blasting method has to be adopted [8] in many cases, which will inevitably cause vibration problem on surrounding rock mass and adjacent structures. For existing tunnels near subway tunneling, possible dynamic damage to their lining should be evaluated before any hazard occurs, especially in the mountainous area Southwest China, where drill-and-blasting is more commonly used.

While developing the public transit systems, associated geohazards such as water and soil ingress, ground surface settlement, and sinkholes are likely to be encountered due to unforeseen ground conditions or other reasons that are not apparent in the preliminary design phase [9–12]. A better mechanical understanding of the effects of the overcrossing tunneling on the existing tunnels would provide a quick but low cost assessment alternative method for evaluating the behavior of underlying tunnels prior to construction.

Dynamic damage or failure during subway blasting excavation might cause fatal damage to surrounding rock mass

and structures. Ren et al. [13] summarized the tectonic structure, geomorphology, hydrogeology, and engineering geology in Guangzhou, China, and reported a collapse of the tunnel face resulting from a blast operation in construction of Guangzhou Subway, which led to a serious sinkhole of 690 m^2, and the collapse of two buildings. Actually, many drill-and-blast practices have been conducted during hydraulic tunnels or mining shafts [14–19], which indicated that blasting vibration has critical influence on damage or failure of surrounding rock mass and lining.

Ma et al. [16] monitored the vibration velocities of surface particles after the blasting of auxiliary holes and showed that vibration isolation can be achieved by the existing blasting cavity. Zhang et al. [20] studied the vibration intensity and frequency at the ejective direction during drill-and-blasting. Dong et al. [21] found that the vibration velocities were different at different points even though the points were in the same distance or elevation to blasting source.

However, fewer research literatures were focusing on the influence of blasting on existing tunnels nearby. Zhao et al. [19] adopted a Finite Element Method (FEM) to study blasting vibration velocity and vibration frequency on existing tunnel. Result shows that field monitoring experiment and numerical simulation can optimize blasting excavation program and provide a reference for other similar engineering projects. Shin et al. [22] studied effect of blast-induced vibration on existing tunnels in soft rocks. Other studies were conducted on damage of surrounding rock mass induced by blasting excavation of adjacent hydraulic tunnels or shafts [17, 23] (Zhao and Long, et al., 2016b), but subway tunnels are usually buried shallower than hydraulic tunnels or shafts.

2. Methodology

The principal purpose of this paper is to carry out a dynamic stability evaluation for underlying tunnels under the influence of drill-and-blast tunneling of an overlying subway tunnel, as a case example for subways with similar situations. Analytical solutions for tunnel bending moment and axial force evaluation are studied by Abate and Massimino [25], and the response of a tunnel lining was expressed as a function of the compressibility and flexibility ratios of the tunnel and the overburden pressure and at-rest coefficient of the earth pressure of the soil. However, for tunnels in irregular shape or complex construction procedure, numerical methods have to be adopted especially for dynamic problems [26].

In recent years, numerical methods such as the finite difference method (FDM) and Finite Element Method (FEM) have been employed to analyze the stress and perform deformation analyses of underground excavations [27, 28] and have been widely employed by researchers to investigate deformations and stress distributions in tunnel intersections and in bifurcation tunnels [29] investigating the influence of a new obliquely crossing tunnel on an existing main tunnel using a 3D finite element analysis. And few investigations have been conducted on dynamic interaction between underground tunnel and ground or adjacent tunnels. Mobaraki and Vaghefi [30] have analyzed the dynamic response of underground tunnel induced by ground blasting. Rebello et al. [31] used FDM to analyze dynamic response of ground structures induced by underground tunnel blasting. Lu et al. [15] adopted FEM to study the dynamic influence on ground airport runway induced by tunnel blasting excavation. It is a growing trend of evaluating dynamic problems in blasting tunneling.

Considering Dynamic Finite Element Method (DFEM) being a more effective measure for this type of dynamic problem, and the most mature and widely adopted in blasting simulation, it is adopted in this study. Given that the coordinate of a particle is X_i $(i = 1, 2, 3)$ at the beginning and x_i $(i = 1, 2, 3)$ at time t, then the motion equation is as follows:

$$x_i = x_i\left(X_j, t\right), \tag{1}$$

with initial condition at $t = 0$ as

$$\begin{aligned} x_i\left(X_j, 0\right) &= X_i \\ \dot{x}\left(X_j, 0\right) &= V_i\left(X_j, 0\right), \end{aligned} \tag{2}$$

where V_i is initial velocity.

In DFEM, explicit equation is adopted as follows:

$$[\mathbf{M}]\,\delta + [\mathbf{C}]\,\dot{\delta} + [\mathbf{K}]\,\ddot{\delta} = \mathbf{P}. \tag{3}$$

where [**M**], [**C**], and [**K**] are mass matrix, damping matrix, and stiffness matrix of the whole system, δ, $\dot{\delta}$, and $\ddot{\delta}$ are displacement vector, velocity vector, and acceleration vector, and **P** is the load vector.

3. Evaluation for Kunming Subway

3.1. Project Overview. The Number 3 Kunming Subway (KS3) tunnel section between Xishan Park Station and Chejiabi Station is designed to be excavated by drill-and-blasting CD method. This section of tunnel is in length of 301.5 m, in radius of 450 m, with inclination of 2‰ from Xishan Park Station to YDK0+535, and with inclination of −28‰ to shield machine well, shown in Figure 1.

This section of subway tunnel is overlying three tunnels, namely, YDK0+492.92 (Newly Built Bijiguan Tunnel, NBB), YDK0+551.61 (Old Pilot Tunnel, OP), and YDK0+578.69 (Expended Bijiguan Tunnel, EB). The top elevations of existing tunnels are, respectively, 7.19 m, 14.5 m, and 6.358 m beneath the tunneling subway bottom. It is obvious that the NBBT has the largest section area and span, so it is chosen as the main object for dynamic evaluation.

Figure 2 shows section contour and dimension of NBBT and geological condition. Mechanical parameters are shown in Table 1. The maximum burial depth of subway tunnel is 20 m, while the minimum is 6.5 m. Main stratas around the tunnel from top to bottom are fully, highly, and intermediary weathered basalt, with RQD from 60% to 80%. And seepage is not obvious in this region.

Table 1: Material parameters.

Type	Natural density/kg/m3	Deformation modulus/GPa	Cohesiveness/kPa	Internal friction angle	Poisson ratio
Plain fill	1.96×10^3	0.035	15	10	0.3
Fully weathered basalt	2.1×10^3	0.055	17	35	0.27
Highly weathered basalt	2.6×10^3	0.075	20	45	0.25
Intermediate weathered basalt	2.7×10^3	9	460	65	0.2
Concrete C35	2.39×10^3	14	4500	62.2	0.3
Concrete C20	2.37×10^3	11	2600	60	0.3

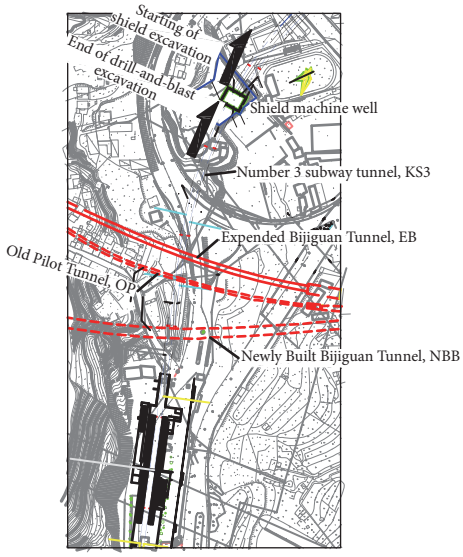

Figure 1: Plan of KS3 tunneling overlying three existing tunnels.

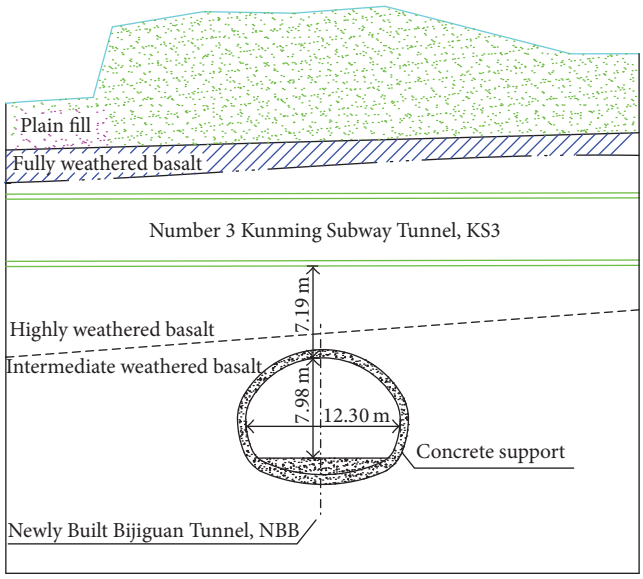

Figure 2: Section contours for underlying NBBT.

Since less weathered basalt is relatively difficult for shield excavation, drill-and-blasting excavation method is considered for this section to shield well. As rock mass between subway tunnel and NBBT is relatively thin, thus drill-and-blasting excavation method would cause vibration on adjacent tunnel, as well as potential damage or even failure. So the stability evaluation during subway tunnel excavation should be carried out on the underlying tunnels. The underlying NBB tunnel is designed as comprehensive lining section, as shown in Figure 2.

3.2. Excavation Method. Since the distance between KS3 and NBB is as small as 7.19 m, it is very difficult to avoid damaging underlying tunnel; thus careful excavation must be adopted in the section of KS3 tunnel near the axis of NBB tunnel. However, the section further away from the axis can still be excavated with other methods so as to accelerate excavation rate.

Section contour of KS3 with full-face excavation is shown in Figure 3, while excavation procedure of CD method is shown in Figure 4. In full-face excavation, most part of the whole contour is formed by one blasting operation, and the inverted arch at the bottom is formed by the second operation. So, most of the time, the step length of full-face excavation is below 3 m, while it is as small as 0.6 m in this

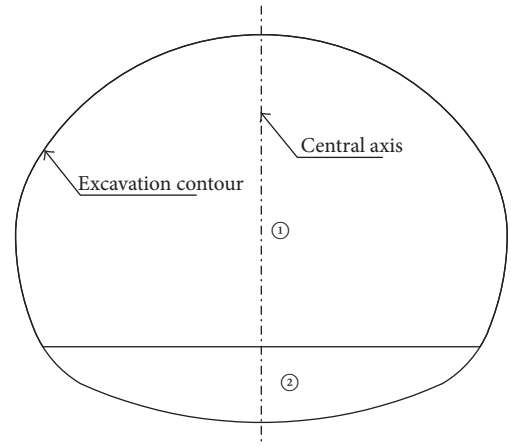

Figure 3: Full-face excavation contours for KS3 subway tunnel.

project. However, in CD method, the section is divided into four parts, which are excavated by four individual blasting operations and temporary supports are installed after each blasting operation. In CD method, excavation area is smaller and supporting makes the tunnel more stable. Temporary support is to be filled with C20 concrete, to enhance its stiffness and strength.

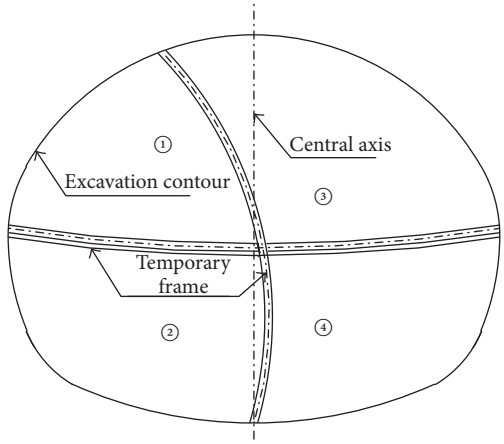

Figure 4: CD method excavation contours for KS3 subway tunnel.

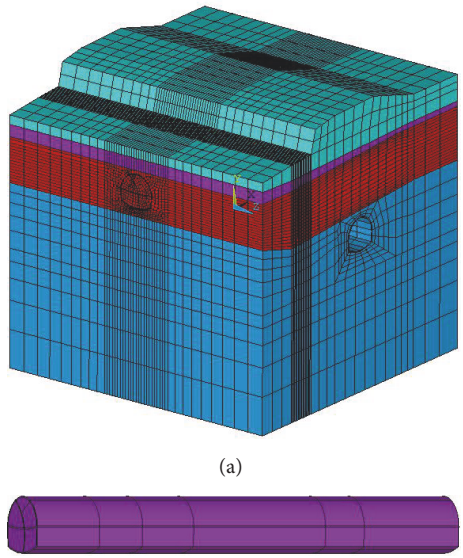

(a)

(b)

Figure 5: Modeling of KS3 subway tunneling over NBBT ((a) model with elements; (b) volume being excavated in subway tunnel).

3.3. Numerical Modeling. Dynamic Finite Element Method (DFEM) is adopted for numerical calculation. The whole model is meshed into 89382 elements and 98210 nodes, shown in Figure 5, and the volume to be excavated includes four different parts in CD method, which can also be considered together as full-face method.

Different layers of strata are modeled according to field investigation result. The topography of ground surface is simplified, since the detail is not significant to numerical calculation focusing on the underground structures.

Four side surfaces and the bottom surface are set as nonreflection surfaces, to simulate the transmission of blast-induced vibration to further field, while the vibration should be reflected at the top surface.

Both existing tunnel lining and surrounding rock were assumed to be elastoplastic materials with incremental stress-strain relations obeying the Mohr-Coulomb yield criteria and associated flow rule. However, all parameters are tested for static calculation, while dynamic parameters are required for calculating blasting influence.

According to the relative study (Zhao and Long, et al., 2016b) the relationship between dynamic elasticity modulus (E_d) and static elasticity modulus (E_s) is as follows:

$$E_d = 8.7577 E_s^{0.5822}. \tag{4}$$

According to the view of Dai [33], in a blasting loading frequency range, the relationship between dynamic Poisson ratio (μ_d) and static Poisson ratio (μ_s) is as follows:

$$\mu_d = 0.8\mu_s. \tag{5}$$

However, during the blasting operation, surrounding rock mass would respond in high strain rate, so it is necessary to consider the high strain rate effect. Therefore, the kinematic hardening constitutive model is adopted. It can be explained by the following equation:

$$\sigma_y = \left[1 + \left(\frac{\dot{\varepsilon}}{C}\right)^{1/p}\right]\left(\sigma_0 + \beta E_p \varepsilon_{\text{eff}}^p\right), \tag{6}$$

where σ_0 is initial yield stress and C and P are Cowper-Symonds strain rate coefficients, relating only to material type. β is a coefficient, where $\beta = 0$ means plastic kinetic hardening and $\beta = 1$ means equivalent hardening model. The static yield stress is the combination of initial yield stress and additional part, $\beta E_p \varepsilon_{\text{eff}}^p$, and E_p is plastic hardening modulus, as in

$$E_P = \frac{E_t E_{\tan}}{E - E_t}, \tag{7}$$

where E_0 is Young's modulus and $E_{\tan}$ is tangent modulus and $\varepsilon_{\text{eff}}^p$ is effective plastic strain and ε_{ij}^p is component plastic strain, which are defined as follows:

$$\begin{aligned} \varepsilon_{\text{eff}}^p &= \int_0^t d\varepsilon_{\text{eff}}^p \\ d\varepsilon_{\text{eff}}^p &= \sqrt{\frac{2}{3} d\varepsilon_{ij}^p d\varepsilon_{ij}^p}. \end{aligned} \tag{8}$$

3.4. Blasting Load Application. After the detonation of explosives, there is a complex thermodynamical process in the borehole, accompanied by shock wave on the borehole wall. Peak load on the borehole wall can be calculated as follows, according to the classical Chapman-Jouguet theory [34]:

$$P_0 = \frac{\rho_0 {V_d}^2}{2(\gamma + 1)} \left(\frac{d_c}{d_b}\right)^{2m} \left(\frac{l_c}{l_b}\right)^m n, \tag{9}$$

where, P_0, ρ_e, V_d, and γ are average initial pressure, density, detonation velocity, and isentropic index of explosive, d_c and d_b are diameter of explosive and borehole, respectively, l_c and

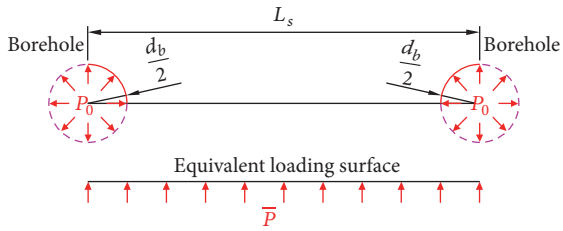

Figure 6: Equivalent application of blasting load.

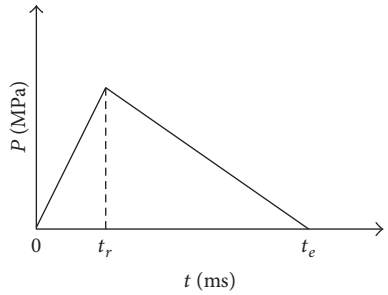

Figure 7: Blasting load applied to excavation contour. (*Note*. Peak load at t_r is 53.6 MPa, and t_r = 2.3 ms and t_r = 17.0 ms, as calculated according to Lu et al. [24].)

l_b are length of borehole and explosive, respectively, and $l_c = l_b$ in shallow borehole blasting. m and n are calculation parameters for loading and should be 3 and 10 for this case.

In standard blasting design, the diameter of boreholes and spacing have the following relationship:

$$L_s = 30d_b. \tag{10}$$

Therefore equivalent blasting load on the line joining holes, shown in Figure 6, is

$$\overline{P} = \delta = \frac{P_0}{30}. \tag{11}$$

And blasting load applied on to the excavation contour is simplified to triangle load as in Figure 7.

All elements are 8-node elements, in average size of 1 m. In this numerical calculation, explicit equations (as (3)) are calculated with Ls-dyna program. And a sensitivity analysis has been carried out on element size, with the same excavation situation of CD method blasting excavation 37 m away. It is indicated that when element size varies from 1 m to 0.2 meters, calculation time is increased by almost 12 times, to 43.5 hours, while vibration response waveforms on monitoring points are quite similar, peak vibration velocity difference is within 2%. Waveforms calculated with different element sizes are compared in Figure 8.

4. Calculation Results and Discussion

4.1. Evaluation Standards. Different countries usually have their own criteria about blasting vibration, such as those specified in AS2187 (Australia, 1983) and DIN 4150 (GOS, 1984). But these standards in developed countries are not updated frequently, while Chinese standard is updated every few years [24]. In most standards vertical vibration velocity is required below 3~8 mm, when frequency is below 10 Hz. According to Chinese "Safety Regulation for Blasting" [32], the vibration limitation for tunnels is listed below in Table 2. And relative safety criteria for lining structures are listed in Table 3.

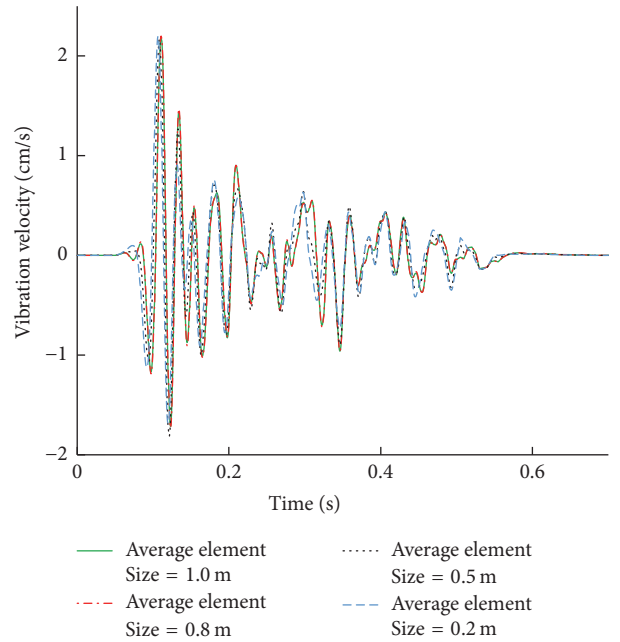

Figure 8: Waveforms calculated with different element sizes.

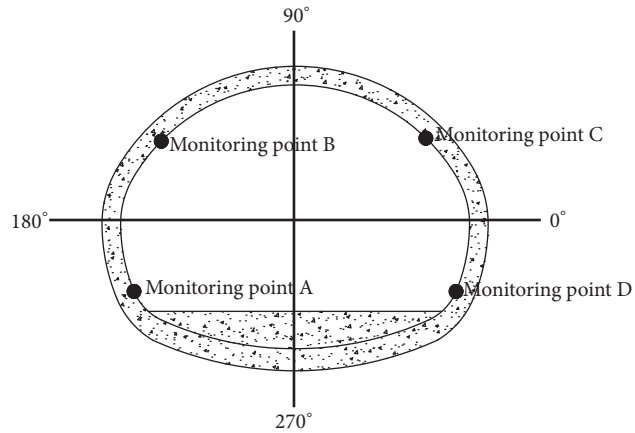

Figure 9: Monitoring points and division on lining of NBB tunnel.

4.2. Vibration on Lining of NBB Tunnel. As the vertical vibration velocity of short footage blasting is larger than the horizontal [35, 36], which conforms calculation result, the vertical vibration velocity is mainly investigated. Furthermore, since concrete is more likely to be damaged by tensile stress, the analysis is focusing on the maximum stress on the lining.

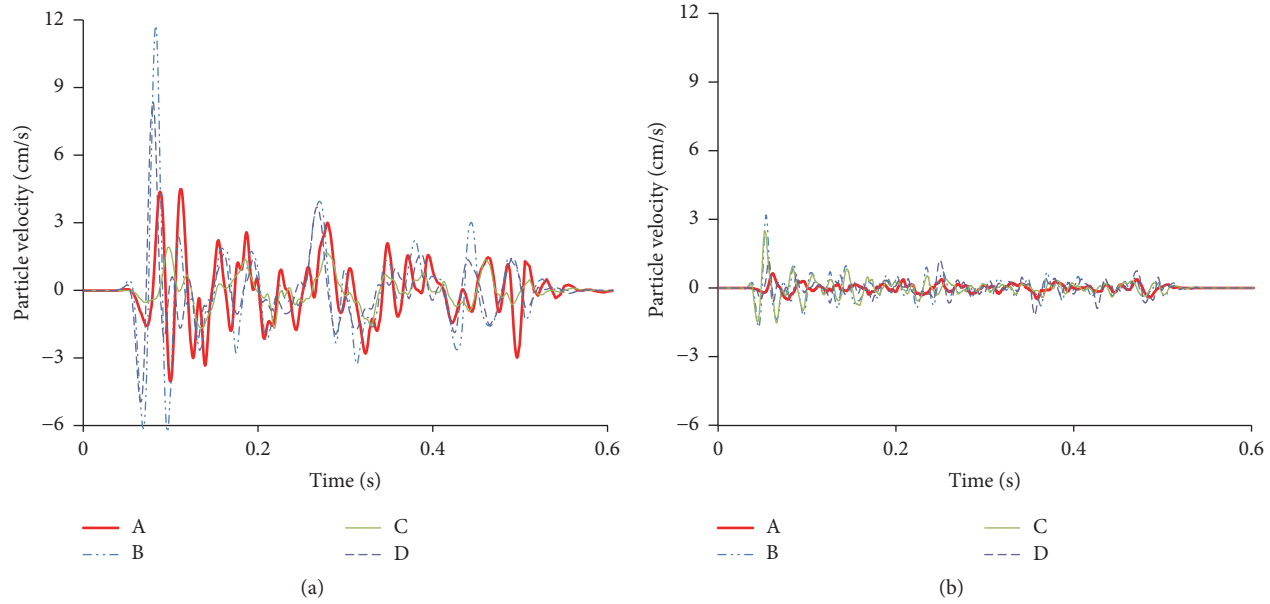

Figure 10: Vertical vibration response on monitoring points induced by full-face blasting (a) and CD method (b).

Table 2: Safety vibration limitation for tunnels and shafts in China [32].

Structure type	Allowable safety peak particle velocity/cm/s		
	$f \leq 10$ Hz	10 Hz $\leq f \leq$ 50 Hz	$f > 50$ Hz
Hydraulic tunnels	7~8	8~10	10~15
Traffic tunnels	10~12	12~15	15~20
Mining shafts	15~18	18~25	20~30

In order to make the analysis more clear, the lining of NBB tunnel is divided into angles and four monitoring points (MP) are focused on as shown in Figure 9, for vertical vibration and dynamic stress response.

Figure 10 shows vertical vibration on lining of NBB tunnel at four different monitoring points, induced by full-face excavation (Figure 10(a)) and Part ③ (shown in Figure 4) of CD method (Figure 10(b)) individually. The blasting source distance in both situations is 37 m from tunnel axis. From Figure 10, it is obvious that largest vibration occurs at MP B in both situations, which is in accordance with the vibration attenuated via distance. However, the peak vibration values induced by full-face blasting or CD method are quite different, with the former being 2.5 times larger. Actually, in blasting operation of Part ③, the blasting contour is no longer a full area, since the left half of the tunnel section is already excavated. Therefore, the perimeters of the blasting counters in two situations are quite different in length, thus making the explosive weight detonated in one delay much less (approximately 40%) than full-face blasting. On the other hand, the free surface on Part ③ is also influencing the propagation of blasting wave, resulting in less vibration velocity on lining of underlying tunnel. It is also interesting that Figure 10 revealed different wave frequencies in both situations, as well as a slight difference in vibration duration.

Comparison shows very large difference in vibration response on lining of the underlying tunnel and suggests that CD method is much safer to adjacent structure.

4.3. Dynamic Stress Variation. Although vibration is considered as evaluation value in most standards, it is tensile stress that controls fundamental damage in dynamical process. Analysis is conducted on dynamical subsidiary stress, as shown in Figure 11.

Comparison between Figures 11(a) and 11(b) also shows advantage of CD method, since the peak value of dynamic tensile stress is approximately only 25% of that induced by full-face blasting. However, different from vibration distribution, the maximum tensile stress on section contour is at MP C. In the radar graph of max tensile stress induced by full-face blasting, shown in Figure 12, the peak tensile stress is located at approximately 65° angle. Actually, this phenomenon is caused by special strata condition of this area, where the subway tunnel is in highly weathered basalt while the underlying tunnel is in intermediate weathered basalt, causing a ratio of 0.075 versus 9 in deformation modulus. This large difference in deformation modulus has influenced the propagation of blast-induced stress wave; thus stress wave reflects at strata boundary and overlaps at MP C with later wave propagating directly from the source.

This process is obvious by observing maximum principle stress distribution versus time, as shown in Figure 13. In the early stage of dynamic stress distribution, the peak tensile stress is at angle of about 270° and then goes to angle of about 330°. But the peak value is about 156.5 ms after detonation. In early stages, tensile stress is not large and is below 1 MPa most of the time. However, the peak value is 1.283 MPa, which just

Table 3: Relevant safety criteria for tunnel lining structures [32].

Structure type	Allowable safety peak particle velocity/cm/s		
	1 d ≤ CA ≤ 3 d	3 d ≤ CA ≤ 7 d	7 d ≤ CA ≤ 28 d
Concrete	1.2	1.2~5.0	5.0~7.0
Shot concrete		5.0	
Grouting	1	1.5	2~2.5
Bolts and anchor cables	1	1.5	5~7

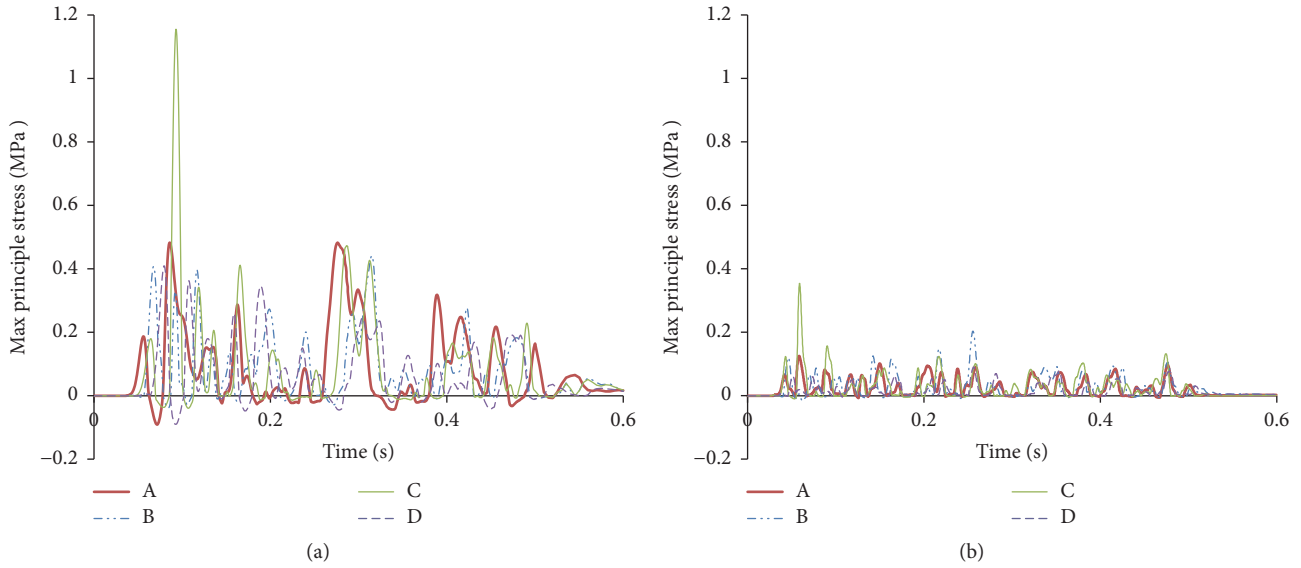

Figure 11: Maximum principle stress response on monitoring points induced by full-face blasting (a) and CD method (b).

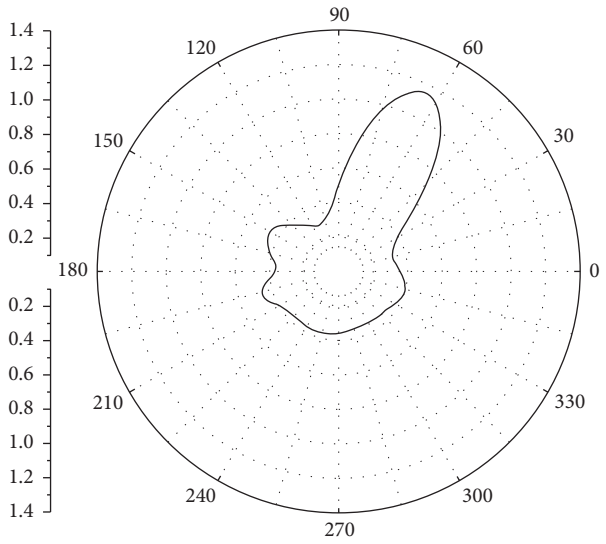

Figure 12: Distribution of peak tensile stress on underlying tunnel induced by full-face blasting.

might cause tensile damage on the lining. Therefore, full-face blasting might be able to apply approximately 40 m beyond the axis of underlying tunnel, with further confirmation from field blasting tests.

Tensile stress distribution variation induced by CD method 25 m away through time is shown in Figure 14, which shows similar peak tensile stress distribution to Figure 13. However, although blasting distance is 33% smaller, the peak tensile stress is only about 50% of that induced by full-face blasting excavation.

More calculations have been carried out to determine a safe distance for CD method and results are listed in Table 4. It is revealed that, even 37 m beyond the blasting source, the vibration induced by full-face excavation reached 12.4 cm/s, which exceeds allowable value of vibration within relevant frequency. So it is reasonable to adopt CD method, in which tunnel section is divided into 4 parts with smaller contour and thus would cause less blasting load on the excavation contour in each blasting operation. Optimized blasting source distance to NBBT should be larger than 12 m and smaller than 25 m.

5. Conclusion

Considering the problem in subway tunneling in mountainous area Southwest China, the number 3 subway construction

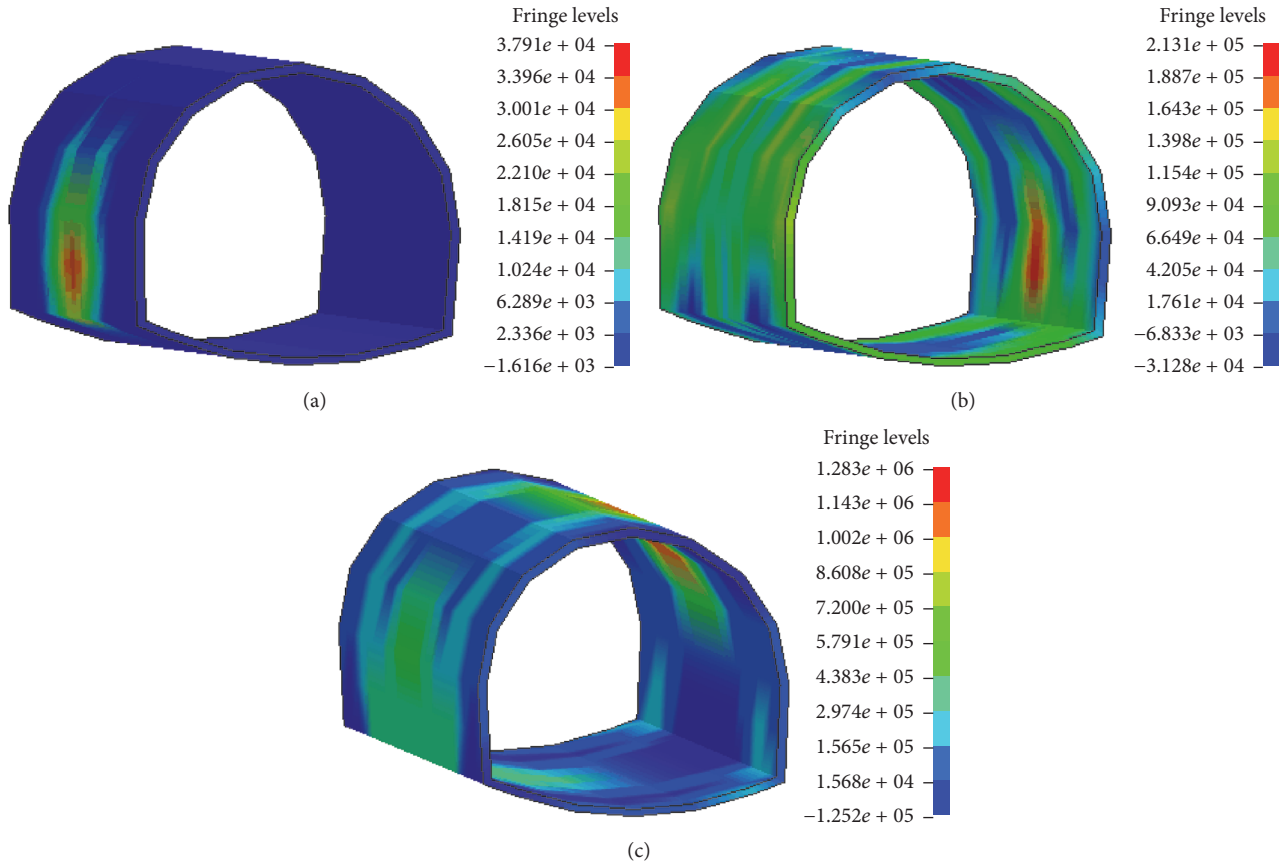

Figure 13: Maximum principle stress distribution variation induced by full-face blasting 37 m away. (*Note*. Positive value for tensile stress. (a) Time = 47.5 ms, (b) time = 91.5 ms, and (c) time = 156.5 ms.)

Table 4: Dynamic response on NBBT lining induced by tunneling.

	Full-face excavation	CD method excavation		
Blasting source distance/m	37	37	25	12
Maximum peak tensile stress/MPa	1.28	0.45	0.63	1.83
Maximum peak particle velocity/cm/s	12.6	3.5	5.8	15.8
Frequency at peak particle velocity/Hz	35.7	54.3	61.1	63.9

in Kunming is taken as a case study. In order to evaluate the potential damage or failure on the existing underlying tunnel, calculations have been carried out with Dynamic Finite Element Method. Following conclusions can be drawn.

Drill-and-blast method would cause different extent of vibration to underlying tunnel depending on specific method and distance between blasting source and object tunnel. Vibration velocity induced by CD method to the underlying tunnel axis is only 28% of that caused by full-face blasting with same distance.

Peak value of tensile stress induced by full-face blasting is capable of causing lining failure at approximately 37 m beyond the underlying tunnel axis. However, CD method has shown much advantage, since blasting within 25 m is also considered safe to the underlying tunnel. But when the blasting source is as near as 12 m beyond the underlying tunnel, the CD method is no longer safe, which still should be confirmed by field blasting tests.

Peak vibration is located on the lining facing the blasting source, while peak tensile stress is on the other side of the contour due to the reflection of stress wave on strata boundary. It is also the key location to be monitored during field blasting tests.

Conflicts of Interest

The authors declare that they have no conflicts of interest.

Acknowledgments

This work was supported by the National Natural Science Foundation of China (51378500 and 51609183) and the Key

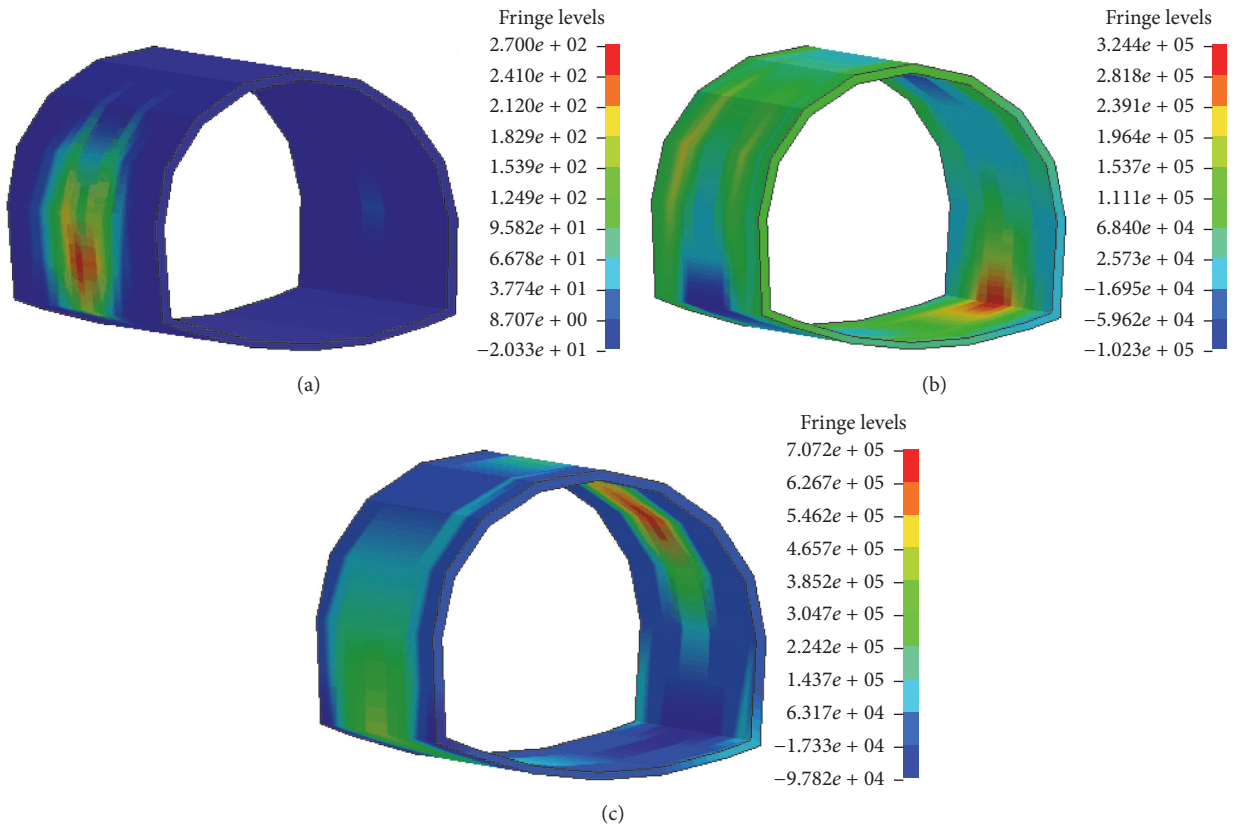

FIGURE 14: Maximum principle stress distribution variation induced by CD method 25 m away. (*Note*. Positive value for tensile stress. (a) Time = 47.5 ms, (b) time = 91.5 ms, and (c) time = 156.5 ms.)

Natural Science Foundation of Hubei Province of China (2015CFA136).

References

[1] S.-L. Shen, H.-N. Wu, Y.-J. Cui, and Z.-Y. Yin, "Long-term settlement behaviour of metro tunnels in the soft deposits of Shanghai," *Tunnelling and Underground Space Technology*, vol. 40, pp. 309–323, 2014.

[2] Y. Tan, X. Li, Z. Kang, J. Liu, and Y. Zhu, "Zoned excavation of an oversized pit close to an existing metro line in stiff clay: case study," *Journal of Performance of Constructed Facilities*, vol. 29, no. 6, article 04014158, 2015.

[3] Z. Guo and N. H. M. Wilson, "Assessing the cost of transfer inconvenience in public transport systems: a case study of the London Underground," *Transportation Research Part A: Policy and Practice*, vol. 45, no. 2, pp. 91–104, 2011.

[4] M. J. M. Maynar and L. E. M. Rodríguez, "Discrete numerical model for analysis of earth pressure balance tunnel excavation," *Journal of Geotechnical and Geoenvironmental Engineering*, vol. 131, no. 10, pp. 1234–1242, 2005.

[5] M. I. Wallace and K. C. Ng, "Development and application of underground space use in Hong Kong," *Tunnelling and Underground Space Technology*, vol. 55, pp. 257–279, 2016.

[6] F. Ji, J. Lu, Y. Shi, and C. Zhou, "Mechanical response of surrounding rock of tunnels constructed with the TBM and drill-blasting method," *Natural Hazards*, vol. 66, no. 2, pp. 545–556, 2013.

[7] H.-N. Wu, S.-L. Shen, S.-M. Liao, and Z.-Y. Yin, "Longitudinal structural modelling of shield tunnels considering shearing dislocation between segmental rings," *Tunnelling and Underground Space Technology*, vol. 50, pp. 317–323, 2015.

[8] B. Li, L. Wu, C. Xu, Q. Zuo, S. Wu, and B. Zhu, "The detection of the boulders in metro tunneling in granite strata using a shield tunneling method and a new method of coping with boulders," *Geotechnical and Geological Engineering*, vol. 34, no. 4, pp. 1155–1169, 2016.

[9] J. Du, R. He, and V. Sugumaran, "Clustering and ontology-based information integration framework for surface subsidence risk mitigation in underground tunnels," *Cluster Computing*, vol. 19, no. 4, pp. 2001–2014, 2016.

[10] R. Liang, T. Xia, Y. Hong, and F. Yu, "Effects of above-crossing tunnelling on the existing shield tunnels," *Tunnelling and Underground Space Technology*, vol. 58, pp. 159–176, 2016.

[11] J. C. Ni and W.-C. Cheng, "Characterising the failure pattern of a station box of taipei rapid transit system (TRTS) and its rehabilitation," *Tunnelling and Underground Space Technology*, vol. 32, pp. 260–272, 2012.

[12] Y.-S. Xu, Y. Yuan, S.-L. Shen, Z.-Y. Yin, H.-N. Wu, and L. Ma, "Investigation into subsidence hazards due to groundwater pumping from Aquifer II in Changzhou, China," *Natural Hazards*, vol. 78, no. 1, pp. 281–296, 2015.

[13] D.-J. Ren, S.-L. Shen, W.-C. Cheng, N. Zhang, and Z.-F. Wang, "Geological formation and geo-hazards during subway construction in Guangzhou," *Environmental Earth Sciences*, vol. 75, no. 11, pp. 1–14, 2016.

[14] J. X. Lai, H. B. Fan, J. X. Chen, J. L. Qiu, and K. Wang, "Blasting vibration monitoring of undercrossing railway tunnel using wireless sensor network," *International Journal of Distributed Sensor Networks*, vol. 2015, Article ID 703980, 7 pages, 2015.

[15] S. Lu, C. Zhou, N. Jiang, and X. Xu, "Effect of excavation blasting in an under-cross tunnel on airport runway," *Geotechnical and Geological Engineering*, vol. 33, no. 4, pp. 973–981, 2015.

[16] H. Ma, H. Wang, C. He, Z. Zhang, and X. Ma, "Influences of Blasting sequence on the vibration velocity of surface particles: a case study of qingdao metro, China," *Geotechnical and Geological Engineering*, vol. 35, no. 1, pp. 485–492, 2017.

[17] P. C. Xu, Q. Dong, X. P. Li, and Y. Luo, "Influence research of underground caverns blasting excavation on excavation damage zone of adjacent cavern," *Advanced Materials Research*, vol. 838-841, pp. 901–906, 2014.

[18] J. Yang, W. Lu, Q. Jiang, C. Yao, S. Jiang, and L. Tian, "A study on the vibration frequency of blasting excavation in highly stressed rock masses," *Rock Mechanics and Rock Engineering*, vol. 49, no. 7, pp. 2825–2843, 2016.

[19] H. B. Zhao, Y. Long, X. H. Li, and L. Lu, "Experimental and numerical investigation of the effect of blast-induced vibration from adjacent tunnel on existing tunnel," *KSCE Journal of Civil Engineering*, vol. 20, no. 1, pp. 431–439, 2016.

[20] N. Zhang, X. Fang, L. Fan, K. Ding, Z. Hua, and P. University, "The influence of initiation sequences on blasting vibration in millisecond blasting," *Explosive Materials*, 2013.

[21] Q. Dong, X. Li, and H. Zhao, "Study on damage characteristic of underground cavern blasting excavation based on dynamic damage constitutive model," in *Proceedings of the International Conference on Advances in Energy, Environment and Chemical Engineering*, Changska, China, September 2015.

[22] J.-H. Shin, H.-G. Moon, and S.-E. Chae, "Effect of blast-induced vibration on existing tunnels in soft rocks," *Tunnelling and Underground Space Technology*, vol. 26, no. 1, pp. 51–61, 2011.

[23] X. Xia, H. B. Li, J. C. Li, B. Liu, and C. Yu, "A case study on rock damage prediction and control method for underground tunnels subjected to adjacent excavation blasting," *Tunnelling and Underground Space Technology*, vol. 35, pp. 1–7, 2013.

[24] W.-B. Lu, Y. Luo, M. Chen, and D.-Q. Shu, "An introduction to Chinese safety regulations for blasting vibration," *Environmental Earth Sciences*, vol. 67, no. 7, pp. 1951–1959, 2012.

[25] G. Abate and M. R. Massimino, "Numerical modelling of the seismic response of a tunnel–soil–aboveground building system in Catania (Italy)," *Bulletin of Earthquake Engineering*, vol. 15, no. 1, pp. 469–491, 2017.

[26] Y. Li, X. Jin, Z. Lv, J. Dong, and J. Guo, "Deformation and mechanical characteristics of tunnel lining in tunnel intersection between subway station tunnel and construction tunnel," *Tunnelling and Underground Space Technology*, vol. 56, pp. 22–33, 2016.

[27] H. Liu, P. Li, and J. Liu, "Numerical investigation of underlying tunnel heave during a new tunnel construction," *Tunnelling and Underground Space Technology*, vol. 26, no. 2, pp. 276–283, 2011.

[28] J. Shi, C. W. W. Ng, and Y. Chen, "Three-dimensional numerical parametric study of the influence of basement excavation on existing tunnel," *Computers and Geotechnics*, vol. 63, pp. 146–158, 2015.

[29] G. M. Gaspari, O. Zanoli, and M. Pescara, "Three-dimensional modelling of the tunnel intersections in weak rock mass on the kadikoy-kartal metro line of istanbul," in *Proceedings of the European Rock Mechanics Symposium, EUROCK 2010*, pp. 491–494, June 2010.

[30] B. Mobaraki and M. Vaghefi, "Effect of the soil type on the dynamic response of a tunnel under surface detonation," *Combustion, Explosion and Shock Waves*, vol. 52, no. 3, pp. 363–370, 2016.

[31] N. E. Rebello, R. Shivashankar, and V. R. Sastry, "Response of strata and buildings to blast induced vibrations in the presence and absence of a tunnel," *Geotechnical and Geological Engineering*, vol. 34, no. 4, pp. 1013–1028, 2016.

[32] Standardization Administration of China. Chinese National Standard GB6722-2014: Safety regulation for blasting. 2015.

[33] J. Dai, *Dynamic Behaviors and Blasting Theory of Rock*, Metallurgical Industry Press, Beijing, China, 2002.

[34] M. Saif, W. Wang, A. Pekalski, M. Levin, and M. I. Radulescu, "Chapman-Jouguet deflagrations and their transition to detonation," *Proceedings of the Combustion Institute*, vol. 36, no. 2, pp. 2771–2779, 2015.

[35] J.-H. Hu, X.-J. Yan, K.-P. Zhou, and L.-H. He, "Study on the deformation and safety in the process of shallow buried tunnel construction," in *Proceedings of the 2009 International Conference on Engineering Computation, ICEC 2009*, pp. 123–126, May 2009.

[36] L. Wang and H. L. Wang, "Influence of different direction vibration peak velocity of tunnel blasting on building," *Blasting*, vol. 29, no. 4, pp. 6–9.